DEVELOPMENT AND VALIDATION OF A GENERALISED ENGINEERING METHODOLOGY FOR THERMAL ANALYSIS OF STRUCTURAL MEMBERS IN FIRE

Hong Liang , Stephen Welch, Tim Stratford & Emmett V. Kinsella

BRE Centre for Fire Safety Engineering, School of Engineering and Electronics, The University of Edinburgh, Edinburgh, EH9 3JL, UK

ABSTRACT

A novel methodology for generalising CFD-based approaches for thermal analysis of protected steelwork in fire has been developed, known as GeniSTELA. This is a quasi-3D approach with computation of a "steel temperature field" parameter in each computational cell. The methodology accommodates both uncertainties in the input parameters and possible variants to the specification by means of parallel calculations. A framework for the inclusion of temperature/time-dependent thermal properties, including the effects of moisture and intumescence, has been established. Indicative values of intumescent material properties have been obtained by means of cone calorimeter testing. These are dependent on initial thickness and exposure heat flux. GeniSTELA has been implemented as a submodel within the SOFIE RANS CFD code. The model is validated against measurements from the BRE large compartment fire tests, which involved well-instrumented post-flashover fires in a 12 x 12m compartment, including steel indicatives with and without protection. Sensitivity studies reveal the expected strong dependencies on structural member specification and properties of protection materials. The computational requirements are addressed, considering aspects such as the number of simultaneous cases and frequency of GeniSTELA call, in order to achieve a reasonable balance between fluid and solid-phase analyses. It is established that the model can be a practical tool, performing c. 10-100 simultaneous thermal calculations before becoming dominant. These steel temperature field predictions provided by GeniSTELA can provide far more flexibility in assessing the thermal response of structures to fire than is available via existing methods.

NOMENCLATURE

c_{ps}, c_{p1}, c_{p2}	specific heat capacity of steel and protection layers 1,2, respectively (J/kg/K)
d	intumescent layer thickness (m)
E_{system}	total energy in the system (J)
h_{c1}, h_{c2}	convection coefficient on sides 1,2, respectively (W/m^2/K)
k_1, k_2	thermal conductivity of protection layers 1,2, respectively (W/m/K)
$\dot{q}''_{net1}$, $\dot{q}''_{net2}$	net heat flux on sides 1,2, respectively (W/m^2)
$\dot{q}''_{r1}$, $\dot{q}''_{r2}$	incident heat flux on sides 1,2, respectively (W/m^2)
t	time (s)
T_{H1}, T_{H2}	gas temperature on sides 1,2, respectively (K)
$T_{1,0}^{(n)}$, $T_{2,0}^{(n)}$	surface temperature at gas/solid interface on sides 1,2 at n^{th} time-step, respectively (K)
T_s, T_1, T_2	average temperatures of steel and protection layers on sides 1,2, respectively (K)
w_{p1}, w_{p2}	"weight factors" of protection layers on sides 1,2, respectively (-)
Δx_s, Δx_1, Δx_2	thickness of steel and protection layers on sides 1,2, respectively (m)
δ_1, δ_2	thermal penetration depth on sides 1,2, respectively (m)
ε_{m1}, ε_{m2}	emissivity of protection layers on sides 1,2, respectively (-)
ρ_s, ρ_1, ρ_2	density of steel and protection layers on sides 1,2, respectively (kg/m^3)
σ	Stefan-Boltzmann constant (5.67x10^{-8} W/m^2/K^4)

INTRODUCTION

Increasing interest in assessing the performance of structures in fire is driving the development of an array of modelling methodologies to be used in fire safety engineering design. Whilst traditionally most code-based design has been invoked simple calculations, referencing measured fire performance in standard tests, the progressive shift towards performance-based design has opened the door to use of advanced methods exploiting numerical models. These approaches will not replace standard testing, but they can already be used in a complementary fashion, to extend the application of test data, or in cases where standard test results are not applicable.

Some simplified modelling methods have also been established, such as the protected member equation in Eurocode 3 (EC3) [1], but as with all semi-empirical methods the results will tend to be conservative and there are of necessity a number of simplifying assumptions. CFD-based methodologies can in principle provide a much more detailed description of the thermal environment and the effects of localised heating, which could be used in conjunction with thermal analysis models to examine structural performance. In previous work [2], a dedicated fine-mesh thermal modelling tool, known as STELA (Solid ThErmaL Analysis), has been implemented with the RANS CFD code SOFIE [3]. However, this research suggests that detailed thermal analysis of structural members in the context of simulations of full-scale building fires remains problematic. This is partly due to the difference of scale between the mesh which can be afforded for the fire and that required for the thermal analysis of the structure, a particular problem with structured meshes, and also the generally high computational demands for coupled analyses. Moreover, existing approaches are limited to consideration of a specific structural arrangement of interest, since it is necessary to define all model parameters in advance. Simulations must be repeated from scratch if details such as the structural geometry or the thermal properties are changed, a very inefficient procedure.

A more general and flexible methodology has now been proposed, still within the context of a CFD fire simulation, as reported elsewhere [4,5]. This is based on computation of a set of "steel temperature field" parameters within the whole of the calculation domain, accommodating, by means of simultaneous calculations, both uncertainties in the input parameters and possible variants to the specification. Hence the need for repeat simulations is bypassed. Furthermore, by predicting the member temperatures at each point in space the limitations of existing methods with regards to the position of the structural component are overcome. Considering the potentially great computational costs associated with the large numbers of thermal analysis calculations required (equal to the number of gas-phase cells times the number of variants studied in the simultaneous calculations), approximate methods are employed to reduce the full 3D thermal response problem down to treatments which are essentially 1D but which include appropriate representations of the heat transfer processes in the other dimensions to reconstruct a quasi-3D solution. This new generalised methodology is called GeniSTELA (Generalised Solid ThErmaL Analysis) and is also implemented in SOFIE [4,5].

The current paper addresses the continued development of this methodology, particularly for intumescent material properties, and analysis of its performance. The validation of GeniSTELA with reference to the full-scale fire tests in the BRE large compartment (12m x12m) is reported [6]. Finally, the computational requirements of GeniSTELA are assessed and discussed.

METHODOLOGY DEVELOPMENT

Brief description

When protected steelwork is exposed to fire, heat is transferred to the structure through a layer of insulation. The transient heating response of the member can in principle be described using conventional methods based on numerical heat transfer. However, full 3D analyses impose great computational demands, due to the large numbers of cells required in order to adequately resolve the steep thermal gradients during the initial heating. Even if the computational resource is available, in simple deterministic models there is no direct mechanism to accommodate uncertainties in the thermal properties and member specification. To overcome these problems, with an appropriate balance

between accuracy and tractability, a novel quasi-3D analysis methodology has been developed [4]. This is achieved by constructing a generalised 1D model and further considering the 2D or 3D effects within the heat transfer processes by appropriate approximations and corrections. The computations are performed in each gas-phase CFD cell in the computational domain.

Generalised 1D model

The generalised 1D model is constructed through analysing the heat transfer to and within an element in an idealised protected steel member assumed to be exposed to heat on two faces, as shown in Fig. 1 below. This element is representative of a slice of a protected steel structure, e.g. a finite section of a flange or a web; two faces are used to allow for situations where the exposure conditions on each side might vary, encompassing also the case of hollow sections with very different exposures on the inside of the structure, though in that case the insulation thickness on the inside is reduced to zero.

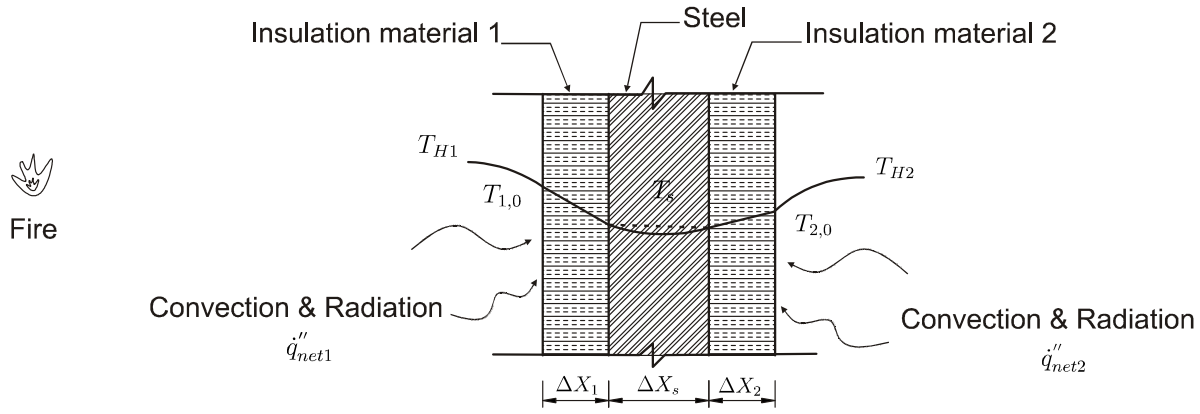

Figure 1. Schematic of heat transfer to protected steel member

The generalised 1D model provides a modelling framework which exploits a simple thermal penetration model for the protection coupled to an essentially lumped parameter representation of the steel heating. The governing equations for this model are derived by considering the net energy balance together with surface heat transfer boundary conditions [7], as given below:

Energy balance equation:

$$\frac{\partial E_{system}}{\partial t} = \dot{q}''_{net}, \text{ i.e. } \rho_s \cdot c_{ps} \cdot \frac{\partial T_s}{\partial t} \cdot \Delta x_s + w_{p1} \cdot \rho_1 \cdot c_{p1} \cdot \frac{\partial T_1}{\partial t} \cdot \Delta x_1 + w_{p2} \cdot \rho_2 \cdot c_{p2} \cdot \frac{\partial T_2}{\partial t} \cdot \Delta x_2 = h_{c1} \times (T_{H1}^{(n)} - T_{1,0}^{(n)}) + \dot{q}''_{r1} - \varepsilon_{m1} \cdot \sigma \cdot T_{1,0}^{(n)4} + h_{c2} \times (T_{H2}^{(n)} - T_{2,0}^{(n)}) + \dot{q}''_{r2} - \varepsilon_{m2} \cdot \sigma \cdot T_{2,0}^{(n)4} \quad (1)$$

The terms shown in the expanded equation here represent, respectively, the transient heating of the steel and protection layer on each side, and the convection, radiation and reradiation for each surface of the protected member. A semi-empirical treatment is adopted for transient heating, allowing for spatially- and temporally-varying temperature gradients within the solid. The boundary conditions are supplied from the heat transfer solution for the surfaces, using the following equations:

$$\dot{q}''_{net1} = \frac{k_1}{w_{p1} \Delta x_1} \cdot (T_{1,0}^{(n)} - T_s), \text{ i.e.: } h_{c1} \times (T_{H1}^{(n)} - T_{1,0}^{(n)}) + \dot{q}''_{r1} - \varepsilon_{m1} \cdot \sigma \cdot T_{1,0}^{(n)4} = \frac{k_1}{w_{p1} \Delta x_1} \cdot (T_{1,0}^{(n)} - T_s) \quad (2)$$

$$\dot{q}''_{net2} = \frac{k_2}{w_{p2} \Delta x_2} \cdot (T_{2,0}^{(n)} - T_s), \text{ i.e.: } h_{c2} \times (T_{H2}^{(n)} - T_{2,0}^{(n)}) + \dot{q}''_{r2} - \varepsilon_{m2} \cdot \sigma \cdot T_{2,0}^{(n)4} = \frac{k_2}{w_{p2} \Delta x_2} \cdot (T_{2,0}^{(n)} - T_s) \quad (3)$$

The weight factors, w_{p1}, w_{p2}, are defined in terms of the thermal penetration depth of the protection:

$$w_{p1} = \min\{\frac{\delta_1}{\Delta x_{p1}}, 1\}\ ,\ w_{p2} = \min\{\frac{\delta_2}{\Delta x_{p2}}, 1\} \tag{4}$$

where:

$$\delta_1 = 2 \cdot \left(\frac{k_1 \cdot t}{c_{p1} \cdot \rho_1} \right)^{1/2}\ ,\ \delta_2 = 2 \cdot \left(\frac{k_2 \cdot t}{c_{p2} \cdot \rho_2} \right)^{1/2}$$

The framework for incorporating temperature/time-dependent characteristics, including moisture and intumescence effects, in the thermal properties descriptions, for generalisation of the methodology, has been described elsewhere [4,5]; further details are provided here on effective intumescent properties, including their derivation from bench-scale tests.

It is well-known that the above situation represents a strongly coupled problem, with the net heat fluxes at the gas-solid interface very much dependent on the surface temperature, but both also related to the transient thermal response of the structure itself. Numerical instabilities might become evident if inadequate solution procedures are used; these are overcome using a Newton-Raphson method to update the surface temperature from the boundary condition governing equations, and thereafter, solving the overall energy balance equation, Eq. (1), with a Runge-Kutta method to obtain the steel temperature; further details are provided in [4].

Quasi-3D model

Use of a fundamentally 1D treatment is essential, considering the costs of doing a full 3D analysis in every computational cell and including a sufficient number of parametric variations. However, adoption of a simple 1D model for thermal analysis could clearly lead to some modelling inaccuracies. In principle, these might be in either direction, resulting in either conservative (over-design) or non-conservative (unsafe) results. The former aspect is not a major concern since the method is in any case far more flexible than other simple models, and by using generalised treatments conservatism is already greatly reduced. The latter aspect is a more obvious problem, and in order to overcome it, methods for treating important 2D and 3D effects are needed. A number of corrections factors have been implemented in the model, encompassing the phenomena indicated in Fig. 2:

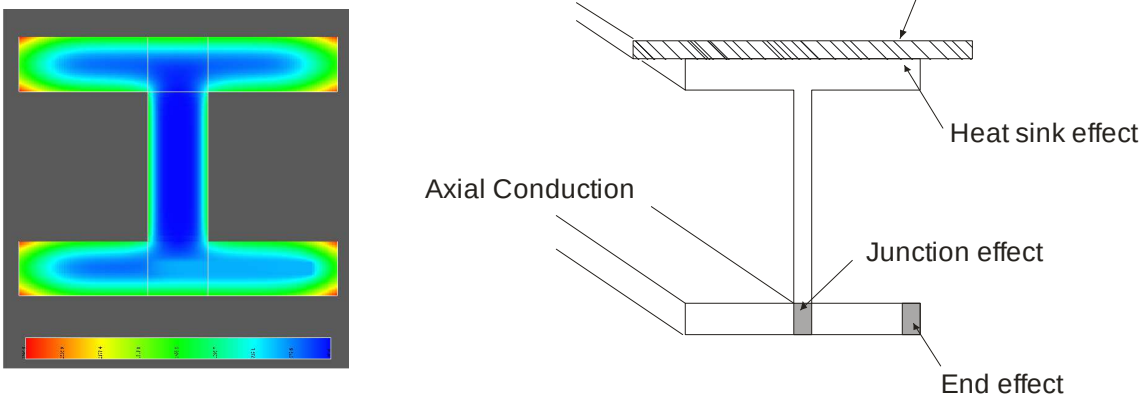

(a) Temperature profile from STELA (b) 3D corrections

Figure 2. Cross-section of the beam with locations of possible correction effects

Specific corrections are made for the “junction effect”, “end effect”, “heat sink effect” and “axial temperature gradient effect”, as described earlier [4]. The significance of these corrections can be found by comparison with the simulation results from other models, e.g. those of STELA, cf. Fig. 2(a). It is important to note that these effects are only critical where they negatively impact the performance of the member, i.e. increase the solid temperatures, and in the majority of cases the opposite is true, i.e. the default procedure is a good representation of the “worst” case. Thus, while it is vital to show that these possible corrections have been appropriately considered, their effect may be relatively minor.

MATERIAL PROPERTIES

The aforementioned model might be considered as a reasonable representation of the *fundamental* aspects of the heat transfer phenomena. However, in practice several factors are found to have a great impact on the transient response, in particular the thermal properties of the protection materials, which affect the surface temperature and thus the steel temperature. It is known that these properties are often strongly temperature/time dependent and the use of constant values may result in significant errors in some cases. The methodology developed here aims at generalising the thermal analysis to accommodate all important phenomena; conventional approaches to treatment of moisture effects have already been implemented, referencing modified specific heats and thermal conductivities [4]. This was later extended further to include the effects of intumescence [5], clearly of great practical relevance to the case of protected steelwork.

Intumescent materials are an increasingly popular form of fire protection, due to a number of advantages arising from the fact that they can be applied as thin, aesthetically pleasing, coatings either before or after construction [8,9,10]. When exposed to high temperatures, they swell and form a layer of carbonaceous char which has much greater thickness than the initial state. The char subsequently acts as a thermal barrier to effectively protect the substrate against increase in temperature. During the process of intumescence, the material properties, such as thermal conductivity, specific heat and density of the intumescent layer, can be severely changed and endo- and exo-thermic reactions occur.

Several research studies have been carried out to determine the effective intumescent thermal properties by experimental tests, in conjunction with some form of numerical analysis. These include bench-scale cone calorimeter tests and small-scale furnace tests on coated plates [11,12], and furnace tests on cellular beams [13]. The bench/small-scale studies examined typical water-based and solvent-containing intumescent systems [11] and later a high-performance material, i.e., epoxy resin containing boric acid and phosphate-based flame retardant [12]. The results from the former showed a significant slow down of temperature increase between 200-300°C, due to intumescence, i.e. the formation of an insulating char and other co-acting energy absorbing processes; temperature influences during the latter tests also resolved a damping effect at 150°C due to the endothermic reaction of boric acid, which also releases water. Layer thickness effects were non-linear.

Considering the effects of geometrical expansion, a simple conceptual model would suggest that thermal equivalence to a finite thickness problem can be achieved by simply scaling the thermal conductivity by the layer thickness, d (=1m), giving an effective thermal conductivity, k/d. Density is scaled in the same way, and specific heat by the inverse of d, but these two parameters always appear as factors of each other, so these scalings vanish in the term ρc_p. The key parameter for the thermal model is therefore the conductivity, or its scaled value, i.e. k/d. The conductivity itself is affected by fundamental changes in the material as it intumesces [11,12,15]. Unfortunately, the effect is non-linear and very dependent on initial thickness, being most pronounced at the smaller thicknesses typical of real applications; hence, there would appear to be no substitute for its direct experimental determination. Here, we have fitted values derived from the results of cone calorimeter tests.

Cone calorimeter tests

Cone calorimeter testing was carried out according to ISO-5660 [16] in order to investigate derivation of the temperature/time-dependent thermal properties of intumescent materials. A single intumescent paint was examined (a white thin-film water-borne coating, Steelguard FM585, supplied by Ameron coatings). It was applied to an Aluminium block, of area 100x100mm by 15mm depth and thermocouples were physically attached (not welded) to the back of the block and at the interface between the block and the intumescent. 12 samples with three intumescent thicknesses (1mm, 2mm, 5mm), together with an uncoated control specimen, were tested at four irradiance levels (30, 60, 75, 90 KW/m^{-2}). Their intumescent expansion ratio was approximated by measuring peak char thickness after the test and their effective thermal conductivity deduced from calibration of a one-dimensional thermal model implemented in a spreadsheet. For this, the conduction heat transfer through the intumescent layer is simply equated to the sensible enthalpy increment of the substrate block, minus a

heat loss term; the latter was scaled from the value deduced for the final conditions of the test (when thermal equilibrium is assumed to apply so that it can be equated to the net heat flux from the cone), weighted by the normalised ratio of the temperature difference between the rear of the block and the ambient conditions. A summary of the results is provided in Table 1 and a photograph of post-test condition of the expanded intumescent material is shown in Fig. 3:

Table 1. Summary of intumescent tests parameters

Test No.	Heat flux (kW/m^2)	Approx. initial thickness (mm)	Approx. final thickness (mm)	Expansion ratio (-)	Nominal *k/d* ($W/m^2/K$)
1	30	1	27	27	30
2	30	2	22	11	23
3	30	5	47	9	18
4	60	1	24	24	28
5	60	2	38	19	20
6	60	5	60	12	12
7	75	1	28	28	25
8	75	2	46	23	15
9	75	5	66	13	10
10	90	1	45	45	20
11	90	2	66	33	12
12	90	5	79	15	9

Figure 3. Photograph illustrating final condition of intumescent in test 5 (2mm, $60kW/m^2$)

The final measured thicknesses in Table 1 show that the overall expansion ratio is not very strongly related to the initial intumescent layer thickness, suggesting that it is mainly the surface material intumescing to creating a thermal barrier. Nevertheless, Figs. 4-6 show that the block temperatures plateaued at lower levels with higher initial thicknesses (shown by the locations of the right-hand ends of the curves), consistent with the fact that greater amounts of intumescent do provide a better insulation effect. The effective (normalised) thermal conductivities are rather variable (and some data points are missing in the lower temperature range for the $60kW/m^2$ plot), but there is a clear trend to lower values at greater thicknesses, consistent with the provision of extra insulation. However, this effect is exposure dependent and Fig. 7 shows a better intumescent performance, i.e. reduced normalised conductivity, at higher fluxes (Test 12) this must be partly due to the relatively greater

expansion thicknesses at high fluxes, hence larger normalising parameter *d*, but other effects may also be relevant. Finally, it should be noted that the intumescent thicknesses used here are greater than typical design specifications for the product tested, due to practical considerations (though c. 1mm is required for some larger members) but this testing was not intended to be a material performance assessment. However, results of this type could in principle be used to provide guidance on representing intumescent thermal properties for use in GeniSTELA for any other products.

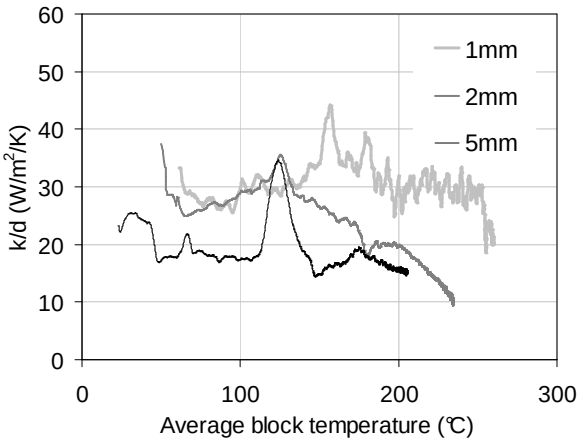

Figure 4. Effective thermal conductivity at 30kW/m^2

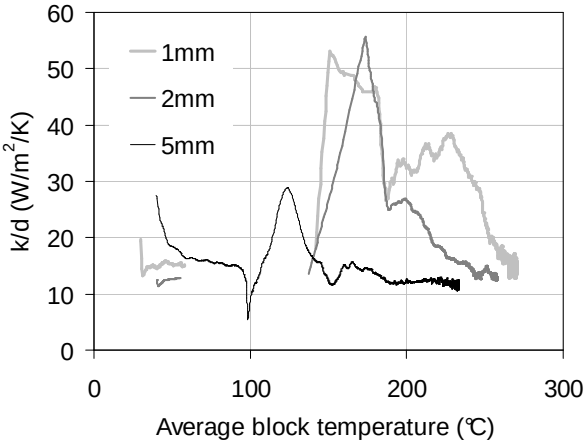

Figure 5. Effective thermal conductivity at 60kW/m^2

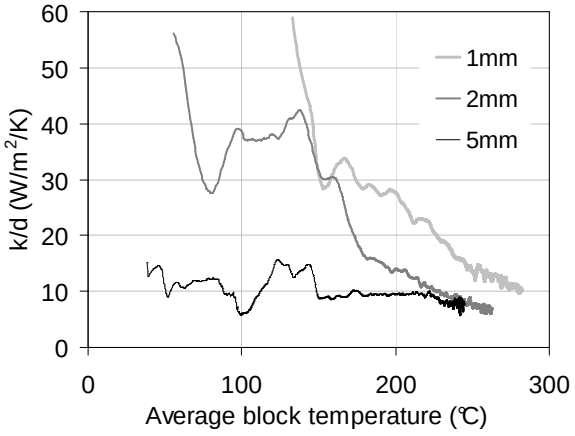

Figure 6. Effective thermal conductivity at 90kW/m^2

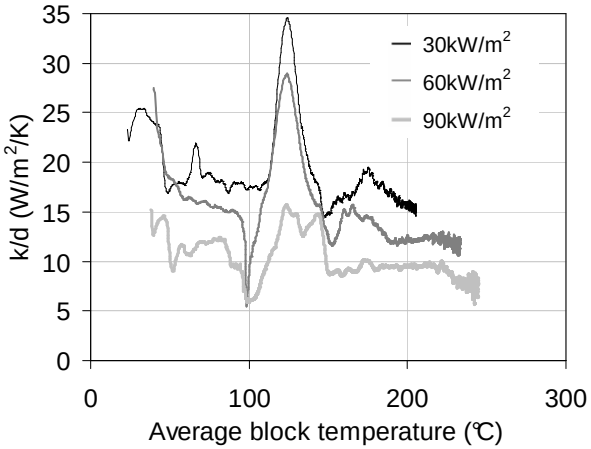

Figure 7. Effective thermal conductivity for 5mm intumescent thickness

MODEL IMPLEMENTATION AND VERIFICATION

The above conceptual model has been implemented as a submodel called GeniSTELA within the SOFIE RANS CFD code [3]. Representative empirical values are adopted for some terms such as the initial conditions, the thermal properties, etc., and their influence has been studied by exercising the model with different sets of input parameter values. The performance of the model was assessed by undertaking sensitivity studies, looking at the effects of a range of numerical and physical parameters. Comparisons were also made with the results from the EC3 protected member equation [1].

The case used for verification studies is the protected steel indicative, UC254x254/73, in the full-scale tests on a 12x12m compartment undertaken at BRE Cardington [17]; this member was protected with about 25mm of Fendolite MII sprayed fibre (baseline ρ=680kg/m^3, k=0.19W/m/K). Fig. 8 shows the fire development stage in the test compartment, while Fig. 9 shows the SOFIE temperature predictions for the fully flashed-over phase of the fire; 48 cribs were used as individual fire sources each with individual burning histories chosen to be in agreement with the measured mass loss data at the 8 load

cells. and according to assumptions about the breakdown of the combustion of the wood and plastic fuels, the latter being allowed to burn off preferentially cf. [17].

In the test a variety of thermal parameter measurements were made, encompassing conditions in the gas phase (temperatures, velocities and heat fluxes) and in the solid phase (steel temperatures in protected beams, columns and indicatives, with and without protection); this study also serves for an initial validation of the model, comparing the model predictions with the measured steel temperatures in the protected indicative.

Figure 8. BRE large compartment fire test

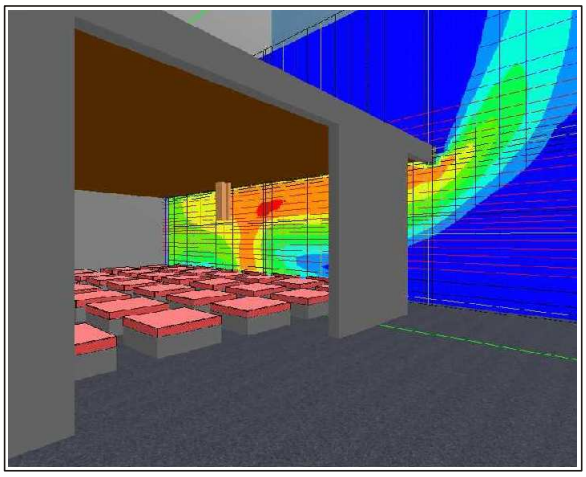

Figure 9. Predicted gas temperature field

Gas and steel temperatures were computed using SOFIE and the coupled GeniSTELA code [4,5]. In qualitative terms the results showed the expected differences in steel and gas temperature fields, with relatively higher steel temperatures within the depth of the compartment compared to the openings. This is consistent with the fact that the thermal exposures are more severe at locations deeper within the fire [17], and the predictions from GeniSTELA are heavily influenced by the radiative terms, $\dot{q}_r''$, derived directly from the SOFIE calculation. Comparison with measured steel temperature and EC3 equation gave a fair agreement, with the latter method giving a more conservative result, c.f. [4,5].

Sensitivity study results

Some results from the sensitivity study are shown in Figs. 10 & 11 for the effects of changing the steel flange thickness (spanning UC 254x254/73,107,167) and different types of protection material. As expected, the change of section factor has a big effect on the heating rate. For the latter case, the two materials were chosen to be thermally equivalent, i.e. they provide the same fire resistance rating, with the initial thickness of the intumescent being about 100 times smaller than for the sprayed fibre. The computed steel temperatures are consistent with this equivalence.

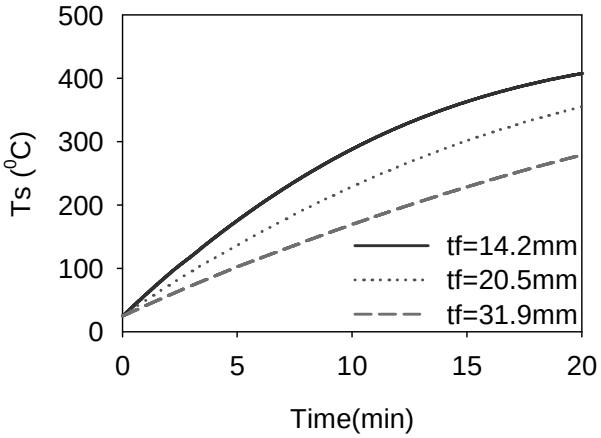

Figure 10. Effect of flange thickness on steel temperature

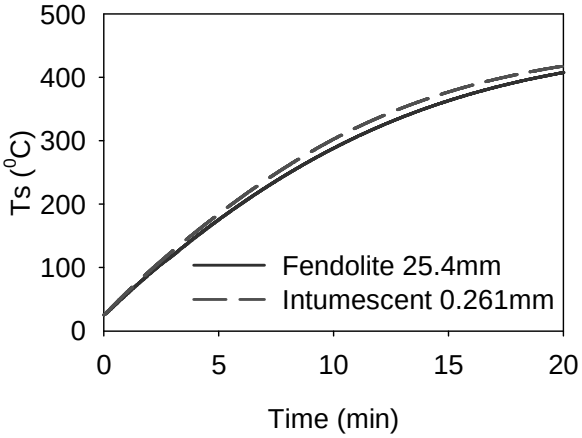

Figure 11. Effect of protection thicknesses on steel temperature

Computational requirements study

The overall computational requirements have been assessed in terms of the CPU time usage. Also, the potential for reducing the frequency of the calls to the GeniSTELA steel temperature solver has been explored by changing this from the default of once every 10 iterations. This default was determined to match the usual frequency of calls to the radiation solver, since one of the key drivers of the thermal response is the radiation field and in most cases there is no benefit in recomputing steel temperatures if this has not been updated. The change in GeniSTELA call frequency is realised by introducing a timestep factor variable (*tfactor*) in the model in order to increase the intervals between calls.

The results showed that GeniSTELA uses around 1% of the CPU time for the flow solver, including radiation, when called at the default interval of 10 iterations. Simulations were then undertaken with a *tfactor* value of 10, for a localised fire scenario, with a constant fire size, having realistic steel temperature increases in 10 minutes. Fig. 12(a) shows the results for the respective steel temperature predictions, confirming that even when called only once per every 100 main solver iterations, i.e. with just six calls of the GeniSTELA solver altogether, there is a very small effect on the final steel temperature result, especially at longer times. Fig. 12(b) shows the evolution of the percentage temperature difference. It is obvious that the discrepancy is only important in the early stage, with the maximum difference being only of order 8%, mostly within 3%. Using an intermediate value of *tfactor*=2 gave results much closer to the default case, with a maximum discrepancy of only 1.5%.

The above findings are of course only of relevance for this particular *steady* fire, and for more general cases, where the heat release rate may be changing rapidly, higher frequencies may be required. In practice, the frequency of the GeniSTELA call could be adjusted by automatic selection linked to heating rates, in order to achieve the best efficiency. Nevertheless, this initial study suggests that a full set of parametric calculations (10-100 cases) could be afforded without any significant compromise of accuracy, before the GeniSTELA analysis becomes the dominant part of the computation.

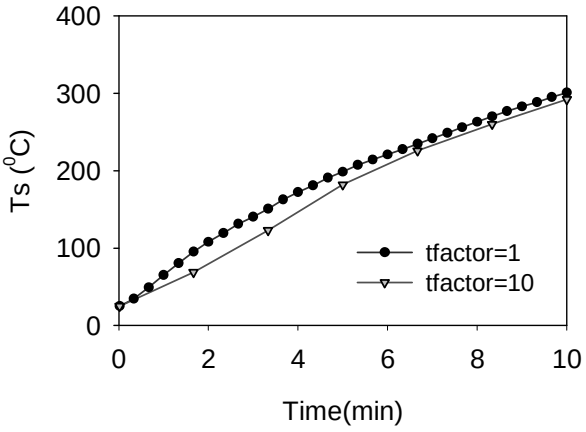

Figure 12a. Predicted steel temperatures with *tfactor*=1 and 10

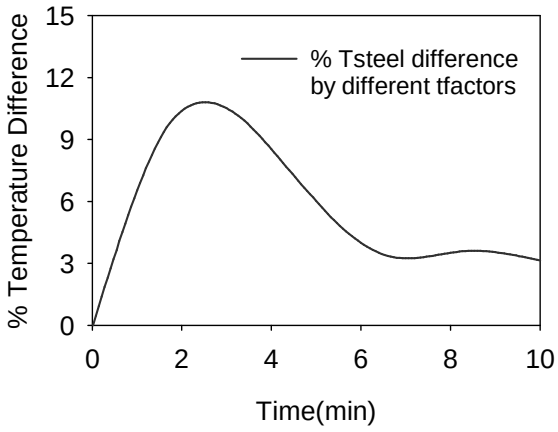

Figure 12b. Difference in steel temperature against time using *tfactor*=1 and 10

CONCLUSIONS

A generalised methodology for thermal analysis of protected steel structures in fire is described. Temperature-dependent properties are adopted, including the effects of moisture and intumescence, and a method by which the latter might be determined has been established, based on bench-scale testing in the cone calorimeter. The GeniSTELA implementation of the method has been extended to simultaneous computations spanning the range of cases of interest; the method has been verified by comparison with data from full-scale tests. Sensitivity studies reveal the expected strong dependencies on structural member specification and properties of protection materials. Computational demands are found to be acceptable, confirming the potential practical use of GeniSTELA. These results serve to illustrate the importance of using generalised methodologies in tackling thermal response problems, providing a possible new approach for performance-based design of steel structures.

ACKNOWLEDGEMENTS

The first author acknowledges the support of her industrial sponsor, the BRE Trust, and the School of Engineering & Electronics. Thanks also to the members of BRE Centre for Fire Safety Engineering, and technical assistants, for their support during the research. Useful comments on intumescent properties were received from Yong Wang and Matthias Bartholmai, and Daniel Joyeux and Mario Fontana via IAFSS email list.

The work reported in this paper has formed part of FireGrid, www.firegrid.org. This research has been funded by the DTI-led Technology Programme along with contributions from the other partners in FireGrid.

REFERENCES

1. British Standards Institution. 2002. Eurocode 3: Design of steel structures – Part 1-2: General rules – Structure fire design.
2. Kumar, S., Welch, S., Miles, S.D., Cajot, L.-G., Haller, M., Ojanguren, M., Barco, J., Hostikka, S., Max, U. & Röhrle, A. 2005. Natural Fire Safety Concept - The development and validation of a CFD-based engineering methodology for evaluating thermal action on steel and composite structures. European Commission Report EUR 21444 EN, 150 pp., ISBN 92-894-9594-4.
3. Lewis, M.J., Moss, J.B. & Rubini, P.A. 1997. CFD modelling of combustion and heat transfer in compartment fires. Proc. 5th Int. Symp. on Fire Safety Science, pp. 463-474.
4. Liang, H. & Welch, S. 2006. A novel engineering tool for thermal analysis of structural members in natural fires. Proc. 4th Int. Workshop on "Structures in fire". Aveiro, Portugal, pp. 287-298.
5. Liang, H. & Welch, S. 2007. Development of an engineering methodology for thermal analysis of protected structural members in fire. Proc. 3rd Int. Conf. on Steel and Composite Structures. Manchester, UK, 30 July - 1 August 2007, pp. 737-743.
6. Lennon, T. & Moore, D. 2003. The natural fire safety concept—full-scale tests at Cardington. Fire Safety Journal, 38, 7, pp. 623-643.
7. Carslaw, H.S. & Jaeger, J.C. 1959. Conduction of Heat in Solids. Oxford University.
8. Goode, M.G. (ed.) 2004 Fire protection of structural steel in high-rise buildings, NIST GCR 04-872.
9. Jimenez, M., Duquesne, S. & Bourbigot, S. 2006. Characterisation of the performance of an intumescent fire protective coating, Surface & Coatings Tech., 201, 3-4, pp. 979-987.
10. Bailey, C.G. 2006a. Advances in fire engineering design of steel structures. Proc. ICE, Structures and Buildings 159, issue SBI, pp. 21-35.
11. Bartholmai, M., Schriever, R. & Schartel, B. 2003 Influence of external heat flux and coating thickness on the thermal properties of two different intumescent coatings using cone calorimeter and numerical analysis, Fire & Materials, 27, 4, pp. 151-162.
12. Bartholmai, M. & Schartel, B. 2007. Assessing the performance of intumescent coatings using bench-scaled cone calorimeter and finite difference simulations. Fire & Materials, 31, 3, pp. 187-205
13. Bailey, C.G. 2006b. Indicative fire tests to investigate the behaviour of cellular beams protected with intumescent coatings, Fire Safety Journal, 36, 8, pp. 689-700.
14. Desanghere, S. & Joyeux, D. 2005. Development of design rules for the fire behaviour of external steel structures. ECSC project no. 7210-PR-380, final report.
15. Tan, K.H., Wang, Z.H. & Au, S.K. 2004. Heat transfer analysis for steelwork insulated by intumescent paint exposed to standard fire conditions. Proc. 3rd Int. Workshop on "structures in fire". Ottawa, Canada, pp. 49-58.
16. British Standards Institution. 1993. ISO 5660-1: Fire tests on building materials and structures – Part 15: Method for measuring the rate of heat release of products.
17. Welch, S., Jowsey, A., Deeny, S., Morgan, R. & Torero, J.L. 2007. BRE large compartment fire tests – characterising post-flashover fires for model validation, Fire Safety Journal, *in press*.